

Metabolome profiling by HRMAS NMR spectroscopy of hyperfunctioning parathyroid glands

Stéphanie Battini¹, Alessio Imperiale^{1,2}, David Taieb³, Karim Elbayed¹, Frédéric Sebag⁴, Laurent Brunaud⁵, and Izzie-Jacques Namer^{1,6}

¹ICube laboratory UMR 7357, University of Strasbourg/CNRS and FMTS, Strasbourg, France, ²University Hospitals of Strasbourg, Department of Biophysics and Nuclear Medicine, Hautepierre, Strasbourg, France, ³La Timone University Hospital, European Center for Research in Medical Imaging, Aix-Marseille University, Marseille, France, ⁴Department of Endocrine Surgery, La Timone University Hospital, Aix-Marseille University, Marseille, France, ⁵Department of Digestive, Hepato-Biliary and Endocrine Surgery, Brabois University Hospital, Nancy, France, ⁶University Hospitals of Strasbourg, Department of Biophysics and Nuclear Medicine, Hautepierre Hospital, Strasbourg, France

Purpose

Primary hyperparathyroidism (pHPT) is a pathologic condition related to the hyperfunction of the parathyroid glands mainly due to a parathyroid adenoma or hyperplasia involving a single gland (single glandular disease, SGD) or more glands (multiple glandular disease, MGD). By contrast, in patients with chronic renal failure or vitamin D deficiency, parathyroid can develop a diffuse hyperplasia related to the physiological secretion of parathyroid hormone in response to hypocalcemia. This affection is commonly called secondary hyperparathyroidism (sHPT). Finally, tertiary hyperparathyroidism (tHPT) is observed in patients with chronic renal failure and long-term sHPT leading to a loss of response to serum calcium levels.

Patients and tumors

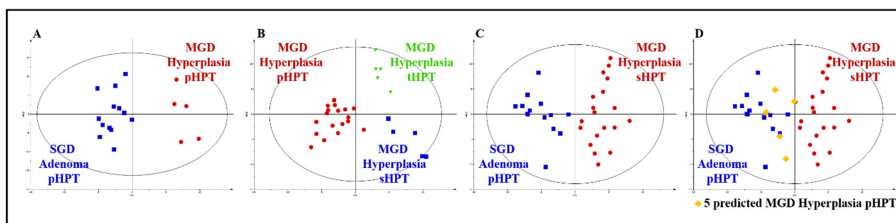
Forty-five samples from thirty-two patients presenting hyperparathyroidism were included in this study: 21 patients (21 samples) with pHPT, 11 patients (19 samples) with sHPT and 3 patients (5 samples) suffering from tHPT. Among the 21 patients with pHPT, 14 patients (14 samples) had SGD and 6 patients (7 samples) had MGD. All the sHPT and tHPT patients presented a MGD. Tumor samples were obtained from 2 institutions in France (La Timone University Hospital, Marseille and Brabois University Hospitals, Nancy). Written informed consent were obtained for all patients.

HRMAS NMR spectroscopy

Tissue specimens were collected during surgery just after tumor removal and were snap-frozen in liquid nitrogen before storage at -80°C . We used frozen tissues for all samples preparation. Each sample was prepared in an environment of -20°C and introduced in a 25 μl disposable Kel-F insert. For each insert, samples were weighted from 15 mg to 20 mg. Next, 4 μl of deuterium oxide with 0.75 weight percent 2,2,3,3-D4-3-(trimethylsilyl) propionic acid, were added in every biopsy's insert to get a chemical shift reference. Just before starting HR-MAS analysis, biopsies' inserts were introduced into 4 mm zirconia rotors. All HR-MAS NMR spectra were achieved on a Bruker Avance III 500 spectrometer which operated at a proton frequency of 500.13 MHz and equipped with a 4mm double resonance gradient HR-MAS probe (^1H and ^{13}C). The spectrometer is installed at the Pathological Department of Strasbourg University Hospitals. The samples' temperature was maintained at 277.15 K throughout the acquisition time, by a Bruker cooling unit (in order to reduce the effects of tissue degradation). Spinning our samples at 3.5 kHz were permitted to reduce as much as possible sidebands out of our region of interest (ROI). In order to minimize the broad signal contributions from lipids and macromolecules, a Carr-Purcell-Meiboom-Gill (CPMG) pulse sequence with pre-saturation of the water signal was used for each sample. A one-dimensional (1D) proton spectrum was acquired for each biopsy's insert. In order to eliminate signal losses due to B_1 inhomogeneity, the inter-pulse delay between the 180° pulses of the CPMG pulse train was synchronized with the sample and set to 285 μs . The number of loops was set to 328, thus giving the CPMG pulse train a total length of 93 ms. The parameters for the CPMG experiment were set as follows: sweep width, 14.2 ppm; number of points, 32k; relaxation delay, 2 s; and acquisition time, 2.3 s. A total of 128 FIDs were acquired resulting in an acquisition time of 10 min. Spectra were referenced by setting the lactate doublet chemical shift to 1.33 ppm. HRMAS NMR signals were bucketed into integral regions 0.01 ppm wide. Moreover, two-dimensional (2D) heteronuclear (^1H - ^{13}C) experiments were performed immediately after the end of 1D spectrum acquisition. We had exclusively acquired only one 2D HR-MAS spectrum by group (because of the tissue's degradation occurs during NMR acquisition). Furthermore, these 2D HR-MAS spectra had confirmed the resonance assignments. To this end, for the metabolites assigning, we had used standard metabolite chemical shift tables available in the literature. Then, data were zero-filled to a 2k * 1k matrix and weighted with a shifted square sine-bell function before Fourier transformation. Finally, 1D HR-MAS spectra were bucketed into integral regions 0.01 ppm wide (ppm range, 6.54-2.32) using AMIX 3.9.14 software (Bruker GmbH, Germany). Then, spectra were exported and analyzed into SIMCA P (version 13.0.3, Umetrics AB, Umeå, Sweden). A combination of PCA and OPLS-DA was herein adopted to evaluate the quality of the data, to identify possible outliers and to optimize the separation between tumor subgroups. Cross-validation was used to determine the number of components and to avoid overfitting the data.

Results and discussion

Significant differences in metabolomic profile were assessed according to both pathologic diagnosis (Adenoma, Hyperplasia) and the type of HPT (primary, secondary, tertiary). A two-component OPLS-DA showed a clear separation between pHPT-related SGD Adenoma and pHPT-related MGD Hyperplasia (A: $\text{R}^2\text{Y} = 0.93$, $\text{Q}^2 = 0.60$) and between pHPT-related MGD Hyperplasia and no primary (secondary and tertiary) HPT-related MGD Hyperplasia (B: $\text{R}^2\text{Y} = 0.78$, $\text{Q}^2 = 0.60$). Moreover, OPLS-DA differentiated pHPT-related SGD Adenoma from sHPT-related MGD Hyperplasia (C: $\text{R}^2\text{Y} = 0.85$, $\text{Q}^2 = 0.64$). We have finally considered the latter model to analyze the main effect between the pathologic origin (Adenoma vs. Hyperplasia) and the functional disease (primary vs. secondary HPT) by considering 5 samples of pHPT-related MGD Hyperplasia. These samples were correctly predicted as pHPT-related adenoma although their sHPT-related hyperplasia origin (D: $\text{R}^2\text{Y} = 0.85$, $\text{Q}^2 = 0.64$).



Our preliminary results show that HRMAS NMR spectroscopy is a reliable method for classifying hyperfunctioning parathyroid lesions in patients with HPT. Moreover, as shown in D, we notice that metabolomic profile of parathyroid glands seems to be less influenced from the histologic origin than the type of HPT, allowing the existence of complex physiopathological mechanisms. The next step analysis is to fully evaluate metabolic profiles (in 1D and 2D analysis) for identifying potential biomarkers involved in the pathogenesis of different entities.

Conclusion

The present study shows that HRMAS NMR could provide new information in the characterization of hyperfunctioning parathyroid glands according to both their histologic origin and the type of HPT. These findings might have clinical and biological implications. However, the real impact of these interesting results should be assessed in long-term prospective studies of a larger cohort of patients.